Proc. Natl. Acad. Sci. USA
Vol. 74, No. 12, pp. 5285–5289, December 1977
Biochemistry

Identification of the major adducts formed by reaction of benzo[*a*]pyrene diol epoxide with DNA *in vitro*

(chemical carcinogens/activation/microsomes/high-resolution mass spectrometry/high-pressure liquid chromatography)

K. M. STRAUB*, T. MEEHAN*, A. L. BURLINGAME†, AND M. CALVIN*

*Laboratory of Chemical Biodynamics and † Space Sciences Laboratory, University of California, Berkeley, California 94720

Contributed by Melvin Calvin, August 31, 1977

ABSTRACT **Covalent binding of the benzo[*a*]pyrene metabolite (±)7β,8α-dihydroxy-9α,10α-epoxy-7,8,9,10-tetrahydrobenzo[*a*]pyrene to calf thymus DNA was investigated. Enzymatic hydrolysis of the carcinogen-modified DNA and subsequent separation via reversed-phase high-pressure liquid chromatography resulted in the detection and isolation of seven distinct products. High-resolution mass spectrometry indicates that these products are covalent adducts of deoxyguanosine, deoxyadenosine, and deoxycytidine. The deoxyguanosine and deoxyadenosine adducts involve binding between the activated hydrocarbon (benzo[*a*]pyrene diol epoxide) and exocyclic amino groups of the respective purines.**

The potent carcinogen benzo[*a*]pyrene (Bz*a*P) undergoes metabolism *in vivo* to a chemically reactive intermediate, which can then react with cellular RNA, DNA, and protein (1, 2). It is widely accepted that these covalent interactions with cellular macromolecules, particularly DNA, are an essential initial step in the process of carcinogenesis (3, 4). Recent work has implicated 7β,8α-dihydroxy-9α,10α-epoxy-7,8,9,10-tetrahydrobenzo[*a*]pyrene (Bz*a*P diol epoxide, Structure I) as the

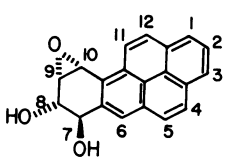

I

molecular species responsible for binding to nucleic acids *in vivo* (5–7).

Weinstein and coworkers have shown that the major RNA adduct found in cell culture is identical to the product obtained by reacting Bz*a*P diol epoxide with poly(G), and involves a covalent bond between C-10 of the hydrocarbon and the N^2 exocyclic amino group of guanine (8, 9). A similar structure has been reported for reaction of the isomeric diol epoxide, 7β,8α-dihydroxy-9β,10β-epoxy-7,8,9,10-tetrahydrobenzo[*a*]pyrene, with poly(G) (10). The structures of the products obtained in the reaction between Bz*a*P diol epoxide and DNA have not been reported, primarily because only microgram quantities of such adducts can be readily isolated from the analogous reaction with DNA.

We have isolated seven distinct products from the reaction of Bz*a*P diol epoxide with calf thymus DNA, and by the use of high-sensitivity, high-resolution mass spectrometry the structures of these products were determined. The results show that adducts are formed between Bz*a*P diol epoxide and the bases guanine, adenine, and cytosine, and involve reactions with the exocyclic amino group of guanine and adenine.

MATERIALS AND METHODS

Adduct Formation and Isolation. Formation of microsomal enzyme-activated Bz*a*P–DNA adducts has been described (11). Racemic Bz*a*P diol epoxide was synthesized as described (12). Diol epoxide (12 nmol/mg of DNA) in 100 μl of dimethylsulfoxide was added to a solution of 100 mg of calf thymus DNA (Sigma Chemical Co.) in 100 ml of 10 mM phosphate buffer (pH 7.2) at 37°. After 24 hr, unbound Bz*a*P diol epoxide and its hydrolysis products were removed by ethyl acetate extraction. The DNA was then precipitated with ethanol and the precipitate was heated to remove intercalated material. The DNA was enzymatically hydrolyzed with deoxyribonuclease II, spleen phosphodiesterase, and alkaline phosphatase (Sigma Chemical Co.), and the modified nucleosides were isolated by Sephadex LH-20 chromatography. This fraction was then further separated by high-pressure liquid chromatography.

High-Pressure Liquid Chromatography. The chromatography was carried out on a Varian model 8500 chromatograph equipped with a Valco injector and two Waters Associates μ-Bondapak C_{18} columns (4.1 mm × 30 cm) connected in series. Fifty percent water/methanol was used as the eluting solvent, at a flow rate of 1 ml/min. A fluorescence detector (Schoeffel Instrument Co.) was used to monitor column effluent; excitation at 248 nm and emission wavelengths greater than 390 nm was used to detect the characteristic 7,8,9,10-tetrahydrobenzo[*a*]pyrene chromophore.

Derivatization Procedure. Each chromatography peak (containing 0.1–1.0 μg of adduct) was collected, taken to dryness, and methylated by the procedure of Hakamori (13). Trimethylsilyl ether derivatives were made by reacting the dried sample with an excess of trimethylsilylimidazole (Pierce Chemical Co.) for 2–3 hr at 100° as described (14).

High-Resolution Mass Spectrometry. Electron impact high-resolution mass spectra were determined by direct probe with a modified Kratos-AEI MS-902 mass spectrometer operated on-line at M/ΔM 10,000 in real-time using a Xerox Sigma 7/LOGOS-II computer system (15, 16).

RESULTS

Modification of DNA and adduct isolation

The covalent binding of Bz*a*P to DNA *in vitro* results in a level of DNA base modification equal to one hydrocarbon adduct per 40,000 nucleotides (2). The microsome-mediated binding conditions used in this work resulted in a similar level of bind-

The costs of publication of this article were defrayed in part by the payment of page charges. This article must therefore be hereby marked "*advertisement*" in accordance with 18 U. S. C. §1734 solely to indicate this fact.

Abbreviations: Bz*a*P, benzo[*a*]pyrene; Bz*a*P diol epoxide, (±)7β,8α-dihydroxy-9α,10α-epoxy-7,8,9,10-tetrahydrobenzo[*a*]pyrene.

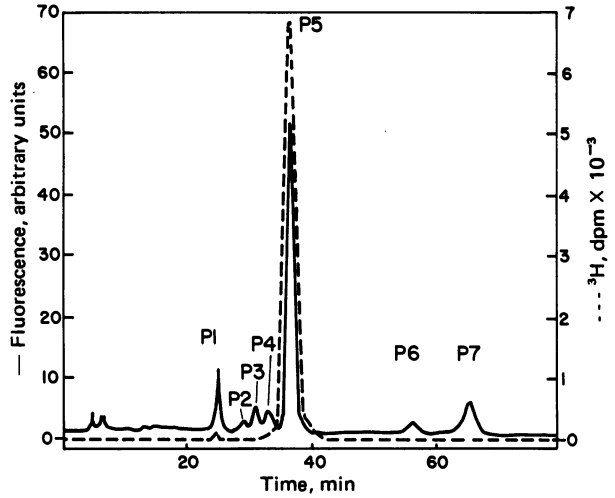

FIG. 1. High-pressure liquid chromatography profile of co-injection of diol epoxide DNA adducts plus adducts obtained from microsome-activated [*G*-^{3}H]Bz*a*P and DNA. The seven major products are labeled P1–P7. Fluorescence units are arbitrary. Full scale for fluorescence represents approximately 50 ng of material.

ing, and Bz*a*P diol epoxide concentrations used (12 nmol/mg of DNA) give a level approximately 5-fold higher. The concentrations of carcinogens and the pH used in these experiments approximate those that could occur *in vivo*. Fig. 1 shows a high-pressure liquid chromatography profile obtained by coinjecting the modified nucleosides derived from Bz*a*P diol epoxide–DNA and microsome-activated [*G*-^{3}H]Bz*a*P–DNA. Seven distinct peaks are evident in the fluorescence trace. A minor component eluting between P5 and P6 was sometimes found but not investigated further in this study. Chromatography of the Bz*a*P diol epoxide–DNA adducts alone results in a fluorescence trace identical to Fig. 1, but chromatography of the microsome-activated Bz*a*P–DNA sample alone resulted in peaks 1, 4, 5, and 7 only. The reaction of Bz*a*P diol epoxide with DNA thus gives three additional products (P2, P3, and P6) not seen in the reaction with microsome-activated Bz*a*P plus DNA. All products exhibit the characteristic fluorescence and absorbance spectrum of 7,8,9,10-tetrahydrobenzo[*a*]-pyrene. Enzymatic hydrolysis of microsome-activated [*G*-^{3}H]Bz*a*P–DNA results in about 40% of the total bound radioactivity eluting from Sephadex LH-20 as Bz*a*P–mononucleosides. The bulk of the remaining unhydrolyzed material exhibits the characteristic fluorescence spectrum of 7,8,9,10-tetrahydrobenzo[*a*]pyrene.

Structure analysis

The structures of P1–P7 were determined by high-resolution mass spectrometry of their permethyl or persilyl derivatives. Verification of elemental compositions for P1, P3, and P5 was obtained by perdeuteriomethylation with CD_3I. The molecular weight of the main component, P5, was also obtained on the underivatized adduct by low-resolution field desorption mass spectrometry.

P1 had a retention time on high-pressure liquid chromatography identical to that of the hydrolysis product of Bz*a*P diol epoxide, Bz*a*P tetraol (7,8,9,10-tetrahydroxy-7,8,9,10-tetrahydrobenzo[*a*]pyrene). High-resolution mass spectrometry of the permethyl and perdeuteriomethyl derivative of P1 gave molecular ions at m/q 376 ($C_{24}H_{24}O_4$) and m/q 388 ($C_{24}H_{12}D_{12}O_4$), respectively. The fragmentation pattern in both cases was identical to that of authentic permethylated Bz*a*P tetraol, obtained by hydrolyzing Bz*a*P diol epoxide in water. Yang *et al.* (17) and Yagi *et al.* (18) have shown that hydrolysis of Bz*a*P diol epoxide gives two isomers, corresponding to *cis* and *trans* addition of water at C-10 of the Bz*a*P diol epoxide. The other Bz*a*P tetraol isomer has a retention time similar to that of P4, and is unresolved from that component.

Table 1. Fragments derived from hydrocarbon moiety of permethylated adducts (P2–P7)

m/q	Elemental composition
345	$C_{23}H_{21}O_3$
344	$C_{23}H_{20}O_3$
313	$C_{22}H_{17}O_2$
312	$C_{22}H_{16}O_2$
298	$C_{21}H_{14}O_2$
297	$C_{21}H_{13}O_2$
282	$C_{21}H_{14}O$
267	$C_{20}H_{11}O$
239	$C_{19}H_{11}$
226	$C_{18}H_{10}$
215	$C_{17}H_{11}$

Fig. 2 shows composite nominal mass plots for the high-resolution mass spectra of permethyl derivatives of P7, P2, and P5. The mass spectrum of permethyl-P6 was identical to that of permethyl-P7; permethyl-P3 was identical to that of permethyl-P5; and permethyl-P4 was identical to permethyl-P2. All six spectra exhibit ions due to fragmentation of the hydrocarbon moiety corresponding to cleavage of the hydrocarbon–nucleoside bond (Table 1), generating the trimethoxytetrahydrobenzo[*a*]pyrene moiety at m/q 345 (composition $C_{23}H_{21}O_3$, ion "a" in Fig. 3). Other ions are then generated by successive loss of the elements of CH_3OH, leading to the aromatized monohydroxybenzo[*a*]pyrene species at m/q 267 ($C_{20}H_{11}O$). This fragment can then lose CO to give the major ion at m/q 239 ($C_{19}H_{11}$). These fragmentation processes are outlined schematically in Fig. 3.

Assignment of the specific purine or pyrimidine in each adduct was deduced from the fragmentation patterns of their respective permethylated derivatives. Von Minden and McCloskey have shown that a major fragmentation pathway of permethylated nucleosides involves cleavage of the C-N glycosidic bond to give a "base + H" ion (19). Table 2 shows the results obtained for permethyl-P2 through P7; in all cases fragments due to the heterocyclic base are of high relative intensity. This allows the assignment of each adduct to a particular nucleoside. Permethyl-P7 (and permethyl-P6) has an intense ion at m/q 149 ($C_6H_7N_5$), corresponding to a monomethyl adenine. Another ion, at m/q 119 ($C_5H_3N_4$), corresponds to loss of the elements of CH_3N from the intact base. Similarly, permethyl-P5 (and permethyl-P3) has an ion at m/q 179 ($C_7H_9ON_5$), indicative of dimethylguanine. This elemental

Table 2. Fragments derived from the nucleoside base moiety of permethylated adducts (P2–P7)

Adduct	m/q	Elemental composition
P2 (P4)	125	$C_5H_7N_3O$
	112	$C_4H_6N_3O$
	111	$C_4H_5N_3O$
P5 (P3)	179	$C_7H_9ON_5$
	150	$C_6H_6ON_4$
P7 (P6)	149	$C_6H_7N_5$
	120	$C_5H_4N_4$

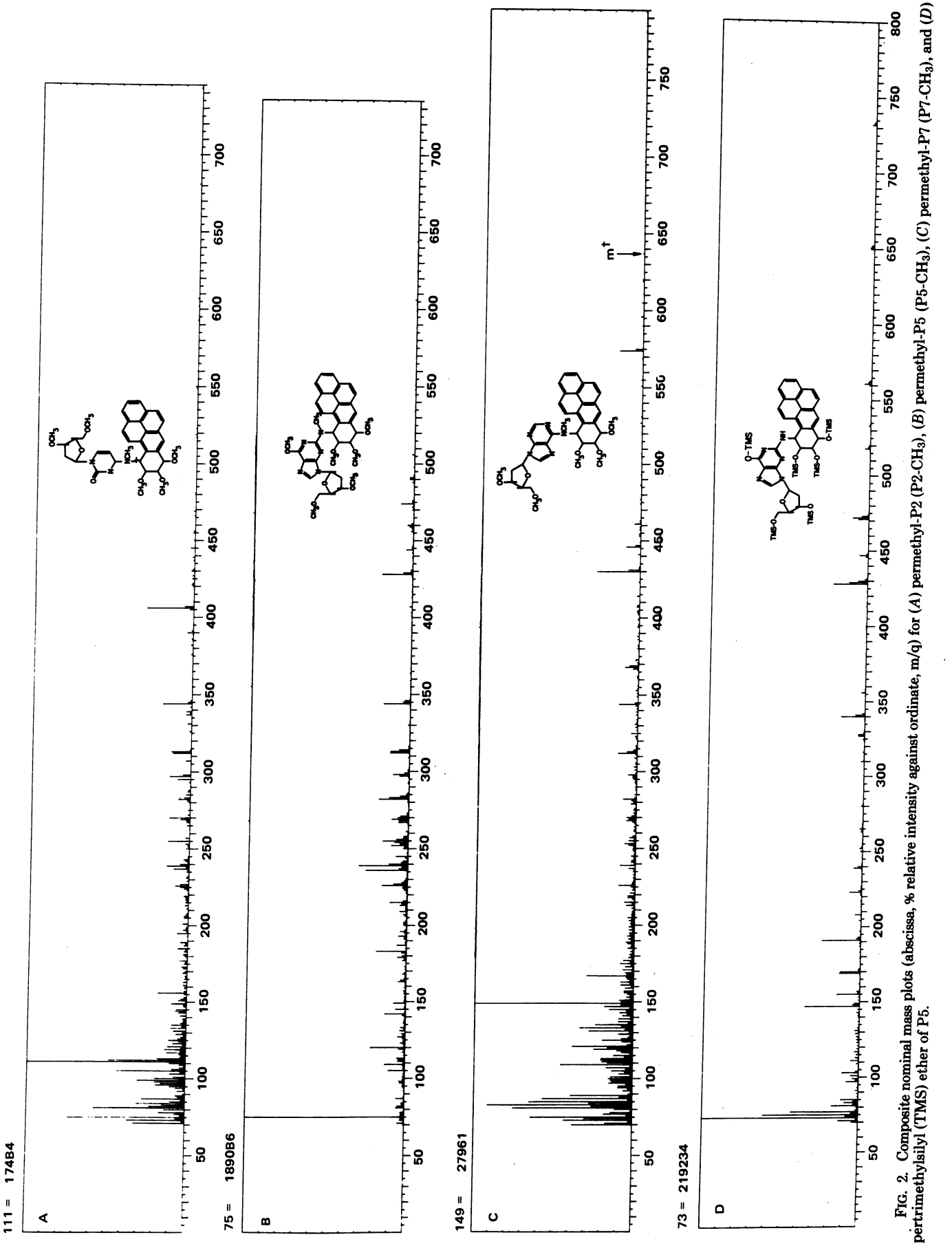

FIG. 2. Composite nominal mass plots (abscissa, % relative intensity against ordinate, m/q) for (*A*) permethyl-P2 (P2-CH_3), (*B*) permethyl-P5 (P5-CH_3), (*C*) permethyl-P7 (P7-CH_3), and (*D*) pertrimethylsilyl (TMS) ether of P5.

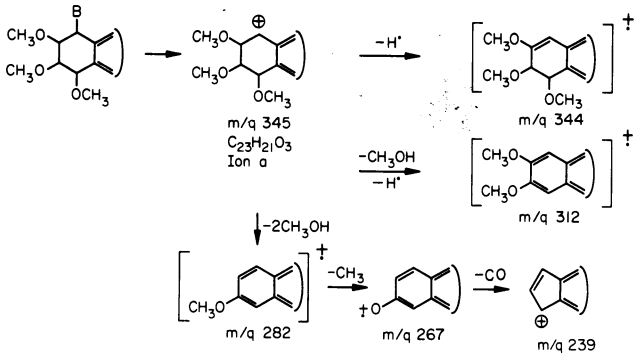

FIG. 3. Schematic fragmentation pathway of the hydrocarbon moiety from a diol epoxide–DNA adduct. "B" refers to a DNA base.

composition was confirmed by perdeuteriomethylation, which gave m/q 185 ($C_7H_3D_6ON_5$). Permethyl-P2 (and permethyl-P4) has a low intensity ion at m/q 125 ($C_5H_7ON_3$) corresponding to monomethylcytosine, with an intense (100% relative intensity) ion at m/q 111 ($C_4H_5ON_3$).

The overall fragmentation for each adduct is dominated by the stability of the aromatic hydrocarbon and purine or pyrimidine moieties. The results obtained for permethyl-P7 serve to illustrate this point. A molecular ion is observed at m/q 637 ($C_{36}H_{39}O_6N_5$). Successive losses of the elements of methanol give m/q 605 ($C_{35}H_{35}O_5N_5$) and 574 ($C_{34}H_{32}O_4N_5$), and loss of the elements of both CH_3OH and the deoxyribose gives m/q 461 ($C_{28}H_{23}O_2N_5$) and 430 ($C_{27}H_{20}ON_5$). Cleavage of this hydrocarbon–purine bond results in the hydrocarbon and base ions discussed above. Permethyl-P2 (and permethyl-P4) gives similar results, except that a molecular ion (expected at m/q 613) is not seen. The highest mass ion, m/q 469 ($C_{28}H_{27}O_4N_3$), corresponds to loss of the deoxyribose from a cytosine–Bz*a*P diol epoxide adduct. Successive losses of the elements of CH_3OH result in m/q 437 ($C_{27}H_{23}O_3N_3$) and 406 ($C_{26}H_{20}O_2N_3$). Cleavage of the hydrocarbon–pyrimidine bond then results in the hydrocarbon and base series of ions.

Von Minden and McCloskey have presented extensive data on the fragmentation patterns of permethylated nucleosides (19). A characteristic ion for permethyl deoxyguanosine, permethyl deoxyadenosine, and permethyl deoxycytidine involves the "base + H" ion (i.e., loss of deoxyribose) which includes a dimethylamino function. This species can then lose methyleneimine (CH_2NH) or the entire dimethylamino function. In the spectra reported here, dimethyladenine or dimethylcytosine ions are not found; only monomethyl species are present. For the adenosine adduct (permethyl-P7), this suggests that direct linkage to the purine (e.g., C-8) does not occur. The occurrence of a relatively low-abundance (1.9% relative intensity) nitrogen-containing hydrocarbon fragment at m/q 279 ($C_{21}H_{13}N$) indicates bonding through the N^6 exocyclic amino group. The apparent high stability associated with the benzylic carbonium ion formed by cleavage of the hydrocarbon–nucleoside bond (ion "a", Fig. 3) explains the relatively low intensity of these nitrogen-containing hydrocarbon fragments. For permethyl-P2 (and permethyl-P4), no such ion can be found, leaving open the possibility of alkylation via the O^2, N-3, or N^4 positions of cytosine.

The major component, permethyl-P5, contains guanine but otherwise follows the same general fragmentation scheme observed for permethyl-P7 and permethyl-P2. High mass ions include m/q 523 ($C_{30}H_{29}O_4N_5$, M^+ − deoxyribose), followed by successive losses of the elements of CH_3OH to give m/q 490 ($C_{29}H_{24}O_3N_5$), 459 ($C_{28}H_{21}O_2N_5$), and the major ion 428 ($C_{27}H_{18}ON_5$, 19.3% relative intensity). Elemental compositions

Table 3. Major fragments found in pertrimethylsilyl (TMS)-P5

m/q	Elemental composition
732	$C_{30}H_{19}O_4N_5(TMS)_3$
651	$C_{25}H_{14}O_3N_5(TMS)_3$
561	$C_{25}H_{13}O_2N_5(TMS)_2$
518	$C_{20}H_{11}O_3(TMS)_3$
472	$C_{25}H_{13}ON_5TMS$
428	$C_{20}H_{10}O_2(TMS)_2$
356	$C_{20}H_{11}O_2TMS$
355	$C_{20}H_{12}ONTMS$
223	$C_5H_4ON_5TMS$

of major ions were confirmed by perdeuteriomethylation with CD_3I. A molecular ion is not observed in the electron-impact spectrum; the highest mass ion that occurs is at m/q 604 ($C_{35}H_{34}O_5N_5$, $M^+ - C_2H_7O_2$). The molecular weight for P5 was therefore obtained by field desorption mass spectrometry. The field desorption spectrum of underivatized P5 consisted of a single peak at m/q 592, corresponding to 569 + Na. The electron impact fragmentation pattern of the base-containing ions does not permit assignment of the alkylation site on guanine. In particular, no nitrogen-containing hydrocarbon ion could be found, making it difficult to distinguish between N^2 or O^6 alkylation. Alkylation at C-8 or other ring positions of the purine would be expected to generate a trimethylguanine species, which was not found. The absence of a Bz*a*P moiety containing nitrogen is again presumably due to the high stability associated with ion "a" (Fig. 3). A persilyl ether derivative of P5 was, therefore, prepared in order to obtain additional structural information. The composite nominal mass spectrum of pertrimethylsilyl-P5 is shown in Fig. 3*D*. Table 3 lists the major ions observed for pertrimethylsilyl-P5. The overall pattern is similar to that of the permethylated derivatives: loss of the deoxyribose followed by successive losses of trimethylsilanol [$(CH_3)_3SiOH$] to give m/q 561 ($C_{31}H_{31}O_2N_5Si_2$). This is then followed by cleavage of the base–hydrocarbon bond to give the base (m/q 223, $C_8H_{13}ON_5Si$) or hydrocarbon series of ions. In this case, however, a relatively low intensity ion corresponding to a nitrogen-containing Bz*a*P species is seen at m/q 355 ($C_{23}H_{21}ONSi$, 0.2% relative intensity). This is consistent with alkylation on the N^2 exocyclic amino group, as was found for alkylation of poly(G) by Bz*a*P diol epoxide (9).

DISCUSSION

The results described in this study are consistent with independent labeling studies which identified P3 and P5 as being guanine adducts, P6 and P7 as adenine adducts, and P4 as probably being a cytosine adduct (11). Interpretation of the mass spectral fragmentation data is most consistent with binding via the exocyclic amino group of adenine and guanine, while cytosine may involve O^2, N-3, or N^4 alkylation. Bonding is presumed to occur at C-10 of the hydrocarbon, since studies have shown that this occurs in the reactions of a wide variety of nucleophiles with Bz*a*P diol epoxide (18, 20). The structures of P2 (P4), P5 (P3), and P7 (P6) are shown as **IV, II, and III,** respectively.

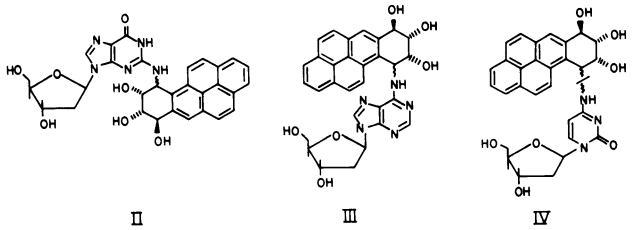

II III IV

The BzaP diol epoxide used in this study was racemic. Enzymatic formation of I is highly stereoselective for a single enantiomer (17, 21, 22) and explains the fact that P2, P3, and P6 were not seen in the adducts obtained from DNA modified by microsome-activated BzaP. P2, P3, and P6 would then correspond to diastereomers of P4, P5, and P7 (one enantiomer of BzaP diol epoxide reacted with the enantiomeric deoxyribonucleoside), and each diastereomeric pair could be expected to give identical electron impact spectra. This explanation is supported by circular dichroism spectra of the adducts (unpublished data, this laboratory). The alternative explanation is that multiple adducts can be formed by *cis* or *trans* addition at C-10 of the hydrocarbon, but model studies suggest that *trans* addition predominates for BzaP diol epoxide (17, 18). Several minor peaks were occasionally observed in the high-pressure liquid chromatogram of these DNA adducts (usually <1% of the reported species) and could be due to products formed by *cis* addition at C-10 or possibly other alkylation sites on the nucleoside bases.

In carrying out analogous experiments with the other geometric isomer of BzaP diol epoxide, 7β,8α-dihydroxy-9β,10β-epoxy-7,8,9,10-tetrahydrobenzo[*a*]pyrene, we have found that the major products do not cochromatograph with the microsome-activated BzaP–DNA adducts represented in Fig. 1.

These results provide an unambiguous determination of the overall molecular structures of the products obtained in the alkylation of DNA by BzaP diol epoxide and extend the available information on alkylation of DNA by polynuclear aromatic carcinogens. Essigman *et al.* have recently reported that the 2,3-oxide of aflatoxin B1 forms covalent adducts with the N-7 of guanine residues (23). 2-Acetylaminofluorene binds to both C-8 and N^2 of guanine (24–26), and both BzaP diol epoxide and synthetic 7,12-dimethylbenz[*a*]anthracene-5,6-oxide bind principally to the N^2 of guanine in poly(G) (27). Adducts with adenine or cytosine in DNA with these polynuclear carcinogens have not been reported. Little is known about the effects of these modifications on DNA structure or how they might alter the functional properties of nucleic acids *in vivo*. BzaP diol epoxide is also capable of catalyzing strand scission in both DNA and RNA, but the physiological significance of this process is not known (28). The results of these binding studies, together with those reported for simple alkylating agents (29), suggest that a multiplicity of sites may be involved in the biological activity of chemical carcinogens.

We thank Mr. Fred Walls for obtaining the high-resolution mass spectra, and Dr. Cedric Shackleton and Mrs. Esther Roitman for preparing the trimethylsilyl derivative. We also thank Dr. H. R. Morris of Imperial College, London, for providing the field desorption mass spectrum. This work was supported in part by the Energy Research and Development Administration, Division of Biological and Environmental Research, and by National Institutes of Health Research Grant RR-00719-03S2 from the Division of Research Resources.

1. Brookes, P. & Lawley, P. D. (1964) *Nature* **202,** 781–784.
2. Gelboin, H. W. (1969) *Cancer Res.* **29,** 1272–1276.
3. Miller, E. C. & Miller, J. A. (1974) in *Molecular Biology of Cancer,* ed. Busch, H. (Academic Press, New York), pp. 377–402.
4. Heidelberger, C. (1975) *Annu. Rev. Biochem.* **44,** 79–121.
5. Sims, P., Grover, P. L., Swaisland, A., Pal, K. & Hewer, A. (1974) *Nature* **252,** 326–328.
6. Ivanovic, V., Geacintov, N. E. & Weinstein, I. B. (1976) *Biochem. Biophys. Res. Commun.* **70,** 1172–1179.
7. Meehan, T., Straub, K. & Calvin, M. (1976) *Proc. Natl. Acad. Sci. USA* **73,** 1437–1441.
8. Weinstein, I. B., Jeffrey, A. M., Jennette, K. W., Blobstein, S. H., Harvey, R. G., Harris, C., Autrup, H. Kasai, H. & Nakanishi, K. (1976) *Science* **193,** 592–595.
9. Jeffrey, A. M., Jennette, K. W., Blobstein, S. H., Weinstein, I. B., Beland, F. A., Harvey, R. G., Kasai, H., Miura, I. & Nakanishi, K. (1976) *J. Am. Chem. Soc.* **98,** 5714–5715.
10. Koreeda, M., Moore, P. D., Yagi, H., Yeh, J. C. H. & Jerina, D. M. (1976) *J. Am. Chem. Soc.* **98,** 6720–6722.
11. Meehan, T., Straub, K. & Calvin, M. (1977) *Nature,* **269,** 725.
12. McCaustland, D. J. & Engel, J. F. (1975) *Tetrahedron Lett.* **30,** 2549–2552.
13. Hakamori, S. (1964) *J. Biochem. (Tokyo)* **55,** 205–208.
14. Axelson, M. & Sjövall, J. (1974) *J. Steroid Biochem.* **5,** 733–738.
15. Burlingame, A. L., Smith, D. H., Merren, T. O. & Olsen, R. W. (1970) "Computers in analytical chemistry," in *Progress in Anal. Chem. Series,* eds. Orr, C. H. & Norris, J. A. (Plenum Press, New York), Vol, 4, pp. 17–38.
16. Burlingame, A. L., Olsen, R. W. & McPherron, R. (1974) in *Advances in Mass Spectrometry,* ed. West, A. R. (Applied Science Publishers, Barking, Essex), Vol. 6, pp. 1053–1059.
17. Yang, S. K., McCourt, D. W., Leutz, J. D. & Gelboin, H. V. (1977) *Science* **196,** 1199–1201.
18. Yagi, H., Thakker, D. R., Hernandez, O., Koreeda, M. & Jerina, D. M. (1977) *J. Am. Chem. Soc.* **99,** 1604–1611.
19. Von Minden, D. L. & McCloskey, J. (1973) *J. Am. Chem. Soc.* **95,** 7480–7490.
20. Beland, F. A. & Harvey, R. G. (1976) *J. Chem. Soc. Chem. Commun.,* 84–85.
21. Nakanishi, K., Kasai, H., Cho, H., Harvey, R. G., Jeffrey, A. M., Jennette, K. W. & Weinstein, I. B. (1977) *J. Am. Chem. Soc.* **99,** 258–260.
22. Yagi, H., Akagi, H., Thakker, D. R., Mah, H. D., Koreeda, M. & Jerina, D. M. (1977) *J. Am. Chem. Soc.* **99,** 2358–2359.
23. Essigman, J. M., Croy, R. G., Nadzan, A. M., Busby, W. F., Reinhold, V. N., Buchi, G. & Wogan, G. N. (1977) *Proc. Natl. Acad. Sci. USA* **74,** 1870–1874.
24. Lin, J. K., Schmall, B., Sharpe, I. D., Miura, I., Miller, J. A. & Miller, E. C. (1975) *Cancer Res.* **35,** 832–843.
25. Lin, J. K., Miller, J. A. & Miller, E. C. (1975) *Cancer Res.* **35,** 844–850.
26. Westra, J. G., Kriek, E. & Hittenhausen, H. (1976) *Chem. Biol. Interact.* **15,** 149–164.
27. Jeffrey, A. M., Blobstein, S. H., Weinstein, I. B., Beland, F. A., Harvey, R. G., Kasai, H. & Nakanishi, K. (1976) *Proc. Natl. Acad. Sci. USA* **73,** 2311–2315.
28. Gamper, H. B., Tung, A. S.-C., Straub, K., Barthomolew, J. C. & Calvin, M. (1977) *Science* **197,** 671–674.
29. Singer, B. (1976) *Nature* **264,** 333–339.